LETTER • OPEN ACCESS

Inter-annual variability of wind and solar electricity generation and capacity values in Texas

To cite this article: Andrew Kumler *et al* 2019 *Environ. Res. Lett.* **14** 044032

View the article online for updates and enhancements.

Recent citations

- The influence of weather regimes on European renewable energy production and demand
Karin van der Wiel *et al*

Environmental Research Letters

LETTER

Inter-annual variability of wind and solar electricity generation and capacity values in Texas

Andrew Kumler[1] , Ignacio Losada Carreño[1,2], Michael T Craig[1] , Bri-Mathias Hodge[1,3], Wesley Cole[1] and Carlo Brancucci[1,3]

1 National Renewable Energy Laboratory, 15013 Denver West Parkway, Golden, CO 80401, United States of America
2 Arizona State University, P.O. Box 875706, Tempe, AZ 85287-5706, United States of America
3 University of Colorado Boulder, 425 UCB, Boulder, CO 80309, United States of America

E-mail: Carlo.Brancucci@nrel.gov

Abstract

As power systems shift towards increasing wind and solar electricity generation, inter-annual variability (IAV) of wind and solar resource and generation will pose increasing challenges to power system planning and operations. To help gauge these challenges to the power system, we quantify IAV of wind and solar resource and electricity generation across the Electric Reliability Council of Texas (ERCOT) power system, then assess the IAV of wind and solar electricity generation during peak-load hours (i.e. IAV of wind and solar capacity values) for the current ERCOT wind and solar generator fleet. To do so, we leverage the long timespan of four reanalysis datasets with the high resolution of grid integration datasets. We find the IAV (quantified as the coefficient of variation) of wind generation ranges from 2.3%–11% across ERCOT, while the IAV of solar generation ranges from 1.7%–5% across ERCOT. We also find significant seasonal and regional variability in the IAV of wind and solar generation, highlighting the importance of considering multiple temporal and spatial scales when planning and operating the power system. In addition, the IAV of the current wind and solar fleets' capacity values (defined as generation during peak-load hours) are larger than the IAV of the same fleets' capacity factors. IAV of annual generation and capacity values of wind and solar could impact operations and planning in several ways, e.g. through annual emissions, meeting emission reduction targets, and investment needs to maintain capacity adequacy.

1. Introduction

In the United States, the installed capacity of solar and wind generators has grown rapidly in recent years, reaching a cumulative 423 and 88 GW in 2017, respectively (US Energy Information Administration 2018). Several factors have driven this growth, including falling wind and solar costs (Barbose *et al* 2016, Lazard 2017, Wiser *et al* 2017) and federal and state policies (US Department of Energy 2017, 2018). Due to economic and policy drivers, wind and solar installed capacity will likely continue to grow (Wiser *et al* 2015, Cole *et al* 2018a, 2018b), with some deep decarbonization scenarios envisioning wind and solar penetrations greater than 60% (Ribera *et al* 2015, Loftus *et al* 2015, Mileva *et al* 2016).

As wind and solar penetrations increase, the variability and uncertainty of wind and solar generation will increasingly impact power system planning and operations. Variability and uncertainty impact the amount of capacity needed to meet planning and operating reserve requirements, and can impact the cost of financing as higher variability can lead to higher project risk. Numerous studies examine how short-term variability and uncertainty impact operations, such as by increasing generator cycling and necessitating increased system reserve requirements (Wan 2011, Lew *et al* 2013, Deetjen *et al* 2017, Zhao *et al* 2017). However, research considering how long-term variability and uncertainty impact planning and operations is lacking. Consequently, here we quantify long-term

variability, specifically inter-annual variability (IAV), of wind and solar resources and generation, and then assess how this IAV might impact system planning and operations.

Prior analyses quantify IAV of wind speed and electricity generation using two types of data: (1) reanalysis datasets, which are coarse but dynamically consistent climate datasets based on unchanging data assimilation schemes and changing data sources, and (2) observations (Li *et al* 2010, Holt and Wang 2012, Wan 2012, Brower *et al* 2013, Rose and Apt 2015). Using 30 years of one reanalysis dataset in the US Great Lakes, Li *et al* (2010) find annual average wind speed IAV exhibits low spatial but high seasonal variability, with greater IAV in winter than summer. Using 24 years of a reanalysis dataset, Brower *et al* (2013) estimate the coefficient of variation (COV) of annual average wind speed IAV ranges from 2% to 6% across the United States. COV quantifies variability around a mean normalized by that mean, i.e. variability of annual average resource around multi-year average resource (see section 2.4 for mathematical definition). Using 32 years of one reanalysis dataset bias-corrected with observations, Rose and Apt (2015) find the COV for annual electricity generation from individual plants ranges from 5% to 12% in the Great Plains, whereas the plants' aggregated generation COV equals 3%.

In addition to using reanalysis and observational datasets (Lohmann *et al* 2006, Markovic *et al* 2009, Pozo-Vázquez *et al* 2011, Davy and Troccoli 2012, Eerme 2012), many studies quantify IAV of solar irradiance and electricity generation using the National Solar Radiation Database (NSRDB) (Gueymard and Wilcox 2011, Madaeni *et al* 2013, Bryce *et al* 2018, Sengupta *et al* 2018), a grid integration dataset that contains high-resolution gridded irradiance data (US National Renewable Energy Laboratory 2017). Using eight years of NSRDB data, Gueymard and Wilcox (2011) estimate the COV of annual average Global Tilt Irradiance (GTI) ranges from 0.5% to 6% and the COV of annual average Direct Normal Irradiance (DNI) ranges from 1% to 10% across the United States. They also find significant seasonal differences in DNI and GTI COV. For instance, the COV of monthly average DNI ranges from 2% to 15% in August and 15% to 30% in February across much of the United States. Using 18 years of NSRDB data for seven sites with observational data, Sengupta *et al* (2018) estimate the COV for annual average Global Horizontal Irradiance (GHI) and DNI ranges from 3% to 5% across sites under all sky conditions.

Overall, prior research suggests the COV of annual average wind speed and solar irradiance ranges from 1% to 5% across the United States, and significantly larger variability exists seasonally and year-to-year. In systems with high renewable penetrations, such variability could significantly affect planning and operations. However, much of the research thus far has quantified variability in wind and solar resource, whereas planning and operations vary with power output. Additionally, existing studies have largely not quantified both wind and solar resource or electricity generation IAV or quantified IAV of metrics relevant to planning and operations. For example, the contribution of wind and solar to meeting peak system demand (called the capacity value) is a key planning metric, and the IAV of capacity value could be much greater than of annual generation because capacity value relies on variation in resource during peak-load hours (Gami *et al* 2017, Cole *et al* 2017). In this study, capacity value is shown as a percentage of nameplate capacity. Using NSRDB and demand data for the Western United States, Madaeni *et al* (2013) find the capacity value of concentrating solar power can range from 15% to 70% across years for a single site. Finally, prior studies have largely quantified resource or generation IAV over regions not aligned with power systems, limiting their applicability to planning and operations.

Here, we quantify the IAV of wind and solar resources and electricity generation in the Electric Reliability Council of Texas (ERCOT) power system. We first quantify IAV of wind and solar resource and electricity generation across all potential wind and solar sites in ERCOT, including by region and season. To link IAV to planning and operations and ground our analysis in a real-world system, we then quantify IAV of capacity values and annual generation of the 2017 ERCOT wind and solar generator fleet. To conduct this analysis, we use reanalysis and grid integration datasets to leverage the advantages of both.

2. Methods

We conduct our study in the ERCOT power system, which serves 90% of Texas' electric load (Electric Reliability Council of Texas 2017a), due to its high wind penetration of 20 GW in 2018 (Electric Reliability Council of Texas 2017c), high wind and solar resource quality (US National Renewable Energy Laboratory 2016), and spatially varied fleet of wind farms (see supplemental information (SI) section SI.1 is available online at stacks.iop.org/ERL/14/044032/mmedia). Solar capacity in ERCOT is expected to reach 1.5 GW in 2018 (Electric Reliability Council of Texas 2017c).

IAV of wind and solar resource varies spatially and temporally (Li *et al* 2010, Gueymard and Wilcox 2011, Wan 2012, Madaeni *et al* 2013, Sengupta *et al* 2018) and manifests on multi-decade timescales (Sengupta *et al* 2018). To account for these factors, we leverage two types of datasets: reanalysis datasets, which span decades but have limited spatial and temporal resolution (table 1), and grid integration datasets, which have a smaller timespan but higher resolution. To take advantage of the multi-decade timespan of reanalysis datasets, we first use them to validate IAV of wind and solar resource in the grid integration datasets. We also validate the grid integration datasets at sub-annual timescales with observed wind and solar data,

Table 1. Summary of reanalysis datasets we use to compare IAV of wind and solar resource in the WIND Toolkit and NSRDB. From each reanalysis, we extract GHI and wind speed.

Reanalysis dataset	Source	Time range	Output spatial resolution	Output temporal resolution
MERRA-1	(Rienecker *et al* 2011)	1979–2016	$0.5° \times 0.667°$ (56 km)	Hourly
MERRA-2	(Gelaro *et al* 2017)	1980-present	$0.5° \times 0.625°$ (50 km)	Hourly
ERA-I	(Dee *et al* 2011)	1979-present	$0.75° \times 0.75°$ (80 km)	3 h
NARR	(Mesinger *et al* 2006)	1979-present	$0.3° \times 0.3°$ (32 km)	3 h

supplementing prior validations (Bañuelos-Ruedas *et al* 2010, Olauson and Bergkvist 2015, Sengupta *et al* 2018). Once validated, we then use the grid integration datasets to explore IAV of wind and solar resource and generation at temporal and spatial scales relevant to power system planning and operations.

We represent wind and solar resource using wind speed and surface GHI, respectively, because they are widely available in reanalysis datasets and are the primary drivers of wind and solar generation. We specifically use 100 m wind speeds because reanalysis datasets provide wind speeds close to 100 m, facilitating accurate approximation using the wind power law (Bañuelos-Ruedas *et al* 2010), and 100 m is a common hub height for modern wind turbines (Draxl *et al* 2015a).

For grid integration datasets, we use the Wind Integration National Dataset (WIND) Toolkit (Draxl *et al* 2015a) and the NSRDB (US National Renewable Energy Laboratory 2017). The WIND Toolkit is a 2×2 km gridded, 5 min resolution dataset covering the continental United States from 2007 to 2013 (Draxl *et al* 2015a). The WIND Toolkit was created with the Weather Research and Forecast Model (WRF) (Skamarock *et al* 2008), a commonly used mesoscale Numerical Weather Prediction model, driven at the boundaries (and initial conditions) by the ERA-Interim reanalysis dataset. While the WIND Toolkit is driven by the ERA-Interim reanalysis, which in turn is used in this comparison, it is still a result of the WRF, where winds are dynamically computed, and thus a different product from reanalysis data. The WIND Toolkit provides meteorological variables, including wind speed, at many hub heights. We focus our analysis on 100 m wind speeds, but test the sensitivity of our results to 80 and 120 m. The NSRDB is a 4×4 km gridded, half-hourly dataset covering the continental United States from 1998 to 2015 (US National Renewable Energy Laboratory 2017). NSRDB downscales satellite-based data using the Physical Solar Model, which runs a radiative transfer model to produce gridded solar radiation. NSRDB provides common solar radiation variables including GHI and Direct Horizontal Irradiance (DHI).

2.1. Validating grid integration datasets
2.1.1. Comparing IAV of grid integration datasets to reanalysis datasets
Given their spatial and temporal completeness, accessibility, and wide use in the literature, we compare the

IAV of the WIND Toolkit and NSRDB with four reanalysis datasets: North American Regional Reanalysis (NARR) (Mesinger *et al* 2006, National Centers for Environmental Prediction 2005), ERA-Interim (ERA-I) (Dee *et al* 2011, European Centre for Medium-Range Weather Forecasts 2009), and Modern-Era Retrospective Analysis for Research and Applications (MERRA) Versions 1 and 2 (Rienecker *et al* 2011, Gelaro *et al* 2017, Global Modeling and Assimilation Office (GMAO) 2008a, 2008b, 2015a, 2015b). Table 1 summarizes key features of each reanalysis dataset. Notably, all reanalysis datasets span over three decades.

Since the reanalysis datasets do not output wind speeds at 100 m, we approximate wind speeds at 100 m (h_{tgt}) at each time step using the wind power law (Kaltschmitt and Wiese 2007) (SI.2). For solar, we use untransformed surface incident solar radiation from each reanalysis, which we assume approximates GHI, and ignore surface albedo.

2.1.2. Validating grid integration datasets at finer timescales
To supplement prior validations with a validation focused specifically on our region of analysis (Draxl *et al* 2015b, Sengupta *et al* 2018), we validate wind and solar resource in the WIND Toolkit and NSRDB, respectively, in Texas. Observed 100 m wind speeds and surface GHI from Bovina (Draxl *et al* 2015b) and Edinburg (Ramos and Andreas 2011), Texas, are analyzed, respectively. Bovina is in the Panhandle along the New Mexico border, whereas Edinburg sits at the southern tip of Texas. Quality-controlled data are available for Bovina from 2009 to 2012 and for Edinburg from 2012 to 2015. We specifically compare average monthly resource between these observed datasets and the data from the nearest grid cell to each location.

2.2. Quantifying IAV of wind and solar resource and electricity generation across ERCOT
After comparing IAV of the WIND Toolkit and NSRDB to that of reanalysis datasets, we use these high-resolution grid integration datasets to quantify IAV of wind and solar resource and electricity generation across ERCOT. To quantify resource IAV, we extract 100 m wind speed and GHI from the WIND Toolkit and NSRDB, respectively. We also test the sensitivity of our results to using 80 and 120 m wind speeds from the WIND Toolkit.

Since system planning and operations vary with electricity generation rather than resource, we also quantify IAV of electricity generation. To do so, we input meteorological data from the WIND Toolkit and NSRDB into the System Advisor Model (SAM), a performance and financial model that converts weather data to wind or solar electricity generation for a specified technology (Blair *et al* 2014). To estimate solar generation, we input DNI, DHI, temperature, and wind speed from NSRDB, and to estimate wind generation, we input wind speed and direction, atmospheric pressure, and temperature from the WIND Toolkit. With respect to technology, we assume fixed tilt solar panels and composite wind turbines of commonly used commercial turbines with 100 m hub height (International Electrotechnical Commission 2005, Draxl *et al* 2015a), but test the sensitivity of our results to 1-axis tracking panels and 80 and 120 m hub heights. For more details, see SI.3. While we do not test the sensitivity of our results to different wind turbine technologies, we found little impact of turbine choice on wind generation in other work (Carreno *et al* in review).

We calculate generation on the native WIND Toolkit and NSRDB grids, then aggregate generation to a common 5.7 × 5.7 km grid (Lopez *et al* 2012). To limit our analysis to areas eligible for wind and solar development, we apply land exclusions for protected land, water bodies (filtering out offshore wind), slope exclusions, and metropolitan areas. These exclusions eliminate small areas in the southwest, northeast, and eastern parts of ERCOT (SI.4).

2.3. Quantifying IAV of wind and solar generation and capacity value of current ERCOT fleet

To better understand real-world planning and operational impacts of wind and solar IAV, we also quantify the potential IAV of the 18.9 GW wind and 0.8 GW solar power capacity installed in ERCOT as of summer 2017 (Electric Reliability Council of Texas 2017d). Specifically, we quantify the IAV of wind and solar power capacity values and electricity generation, key metrics relevant to planning and operations, respectively. Capacity value indicates the fraction of a generator's capacity available during peak demand periods. As such, it determines generators' contributions to resource adequacy, i.e. to ensuring sufficient capacity exists to meet peak demand plus a planning margin. Many utilities and system operators, including ERCOT, utilize this reliability metric during planning (PJM Interconnect 2017, Electric Reliability Council of Texas 2017b).

To isolate resource-induced IAV and to control for wind and solar growth over the last decade, we estimate historic wind and solar generation of the 2017 ERCOT fleet by inputting WIND Toolkit and NSRDB meteorological data into SAM (see section 2.2). Since

ERCOT only provides the county of wind and solar plants, we estimate each plant's hourly historic resource as the average hourly resource for all grid cells overlaying that plant's county. We then sum generation across plants to estimate generation by all wind and solar farms.

To estimate capacity values, we use ERCOT's current method to quantify real-world IAV consequences (Electric Reliability Council of Texas 2017b). However, many methods to calculate capacity value exist (Milligan *et al* 2017), and future research should explore the sensitivity of capacity value IAV to different calculation methods. Per ERCOT's method, we calculate winter and summer capacity values as generation coincident with the top 20 demand hours in the winter (December–February) and summer (June–August). ERCOT publishes hourly load through 2014 (Electric Reliability Council of Texas 2018b). Consequently, we estimate solar generation and capacity values for 2002–2014 (limited by contiguous peak-load data and NSRDB timespans) and wind generation and capacity values from 2007–2012 (limited by the WIND Toolkit's timespan). Over this period, summer peak load consistently occurs between 3 and 7 p.m., while peak winter load consistently occurs between 6 a.m. and 2 p.m. and between 6 and 11 p.m. (SI.5). Thus, wind and solar capacity value IAV in our analysis is attributable to wind and solar generation IAV, not demand variability, as capacity values do not depend on the magnitude of peak load but rather the timing.

2.4. Coefficient of variation

To quantify the IAV of wind and solar resource, electricity generation, and capacity values, we use the COV. In general, the COV equals the multi-year standard deviation divided by the multi-year mean:

$$\text{COV} = \frac{\sqrt{\frac{\sum_{i=1}^{N}(x_i - \overline{x})^2}{N-1}}}{\overline{x}} * 100\,\%, \tag{1}$$

where *i* indexes year; x = single-year mean for a given temporal and spatial scale; $\overline{x}$ = multi-year mean for a given temporal and spatial scale; and N = number of years. We quantify COV over several spatial and temporal scales, as summarized in table 2. Since COV quantifies variability around the mean normalized by the mean, it facilitates comparison of variability across differing average resource (or generation) levels.

3. Results

3.1. IAV of ERCOT-wide wind resource and electricity generation

3.1.1. Comparing wind speeds from WIND toolkit to reanalysis datasets and observations

We leverage the multi-decade timespan of the reanalysis datasets to assess IAV of wind speeds from the

Table 2. Temporal and spatial scale and relevant results section of each COV analysis we perform.

Type of COV	Temporal scale	Spatial scale	Results sections
Annual generation, ERCOT-wide	Annual	ERCOT	3.1.2, 3.2.2
Seasonal generation, ERCOT-wide	Seasonal	ERCOT	3.1.2, 3.2.2
Regional generation, ERCOT-wide	Annual	Regional	3.1.2, 3.2.2
Annual generation, current ERCOT fleet	Annual	Counties with wind or solar in current ERCOT fleet	3.3.1
Seasonal generation, current ERCOT fleet	Seasonal	Counties with wind or solar in current ERCOT fleet	3.3.1
Capacity values, current ERCOT fleet	Annual	Counties with wind or solar in current ERCOT fleet	3.3.2

WIND Toolkit. Annual average wind speed has a similar COV in the WIND Toolkit (3.0%) as the reanalysis datasets (2.4%, 2.9%, 3.2%, and 3.4%), despite the WIND Toolkit's shorter timespan (SI.6). Additionally, average annual wind speeds have a similar range in the WIND Toolkit ($0.7 \, \mathrm{m \, s^{-1}}$) as in most reanalysis datasets (0.6, 0.8, 0.8, and $1.1 \, \mathrm{m \, s^{-1}}$). Thus, the WIND Toolkit provides a reasonable approximation of wind speed IAV despite its sub-decadal timespan. Using observational data, we also find the WIND Toolkit reasonably approximates sub-annual wind speeds (SI.6).

3.1.2. Spatial and temporal variability in average and IAV of wind speed and generation
Given that the WIND Toolkit largely captures wind speed IAV and has a higher spatial and temporal resolution than reanalysis datasets, we use the WIND Toolkit to examine spatial and temporal variability in wind speed and electricity generation and their IAV for every grid cell throughout Texas. We represent electricity generation as capacity factors, or generation normalized by maximum potential generation.

Average annual wind speed and capacity factors generally share a similar spatial distribution, with high values through central Texas and lower values through eastern Texas (figure 1). IAV of wind speed and capacity factors also share similar spatial distributions. IAV is inversely proportional to average speed and capacity factor, e.g. low IAVs coincide with high wind speeds and capacity factors in central and western Texas. Since the cube of wind speeds drives wind generation, capacity factor IAV (2.3%–11%) is greater than wind speed IAV (1.1%–6%). Increasing hub height from 80 to 120 m increases mean capacity factors by about three percentage points with negligible increase in COV, indicating higher hub heights would yield higher generation but similar variability (SI.7).

Given regional transmission constraints and operational differences across seasons, we quantify IAV by region and season. Based on ERCOT's load zones, we divide ERCOT into Panhandle, West, North, South, and Houston regions (SI.8) (Electric Reliability Council of Texas 2018a). To capture IAV at the regional and seasonal level, we estimate the average seasonal and regional COV for each grid cell, then aggregate grid cells into distributions (figure 2). Thus, each region's distribution includes the COV of annual average capacity factors of each grid cell in that region, whereas each season's distribution includes the COV of average capacity factors for that season of each grid cell in ERCOT.

Large seasonal heterogeneity exists in the IAV of capacity factors. Spring exhibits the highest median IAV (12.2%), nearly twice as much as fall and summer, which exhibit the lowest median IAV (7.3% and 7.7%, respectively). Notably, each season has a higher COV than all seasons combined (5.5%), underscoring the need to consider IAV at sub-annual timescales. Within a given season, COVs vary by up to four times across ERCOT. For instance, in summer and spring, COVs range from 2% to 19% and 4% to 19%, respectively.

Capacity factor IAV also varies significantly across regions. The Houston region exhibits the highest median IAV (8.7%), or more than twice as much as the Panhandle (4.0%), which has the lowest median IAV across regions. Furthermore, the Panhandle region has lower median IAV than all of ERCOT (5.5%). In general, regions with greater wind resources have lower IAVs. IAV also varies significantly within each region, reflecting regions' sizes and resource diversity. Shifting hub height from 100 m to 80 or 120 m has a negligible impact on regional and seasonal IAV (SI.7).
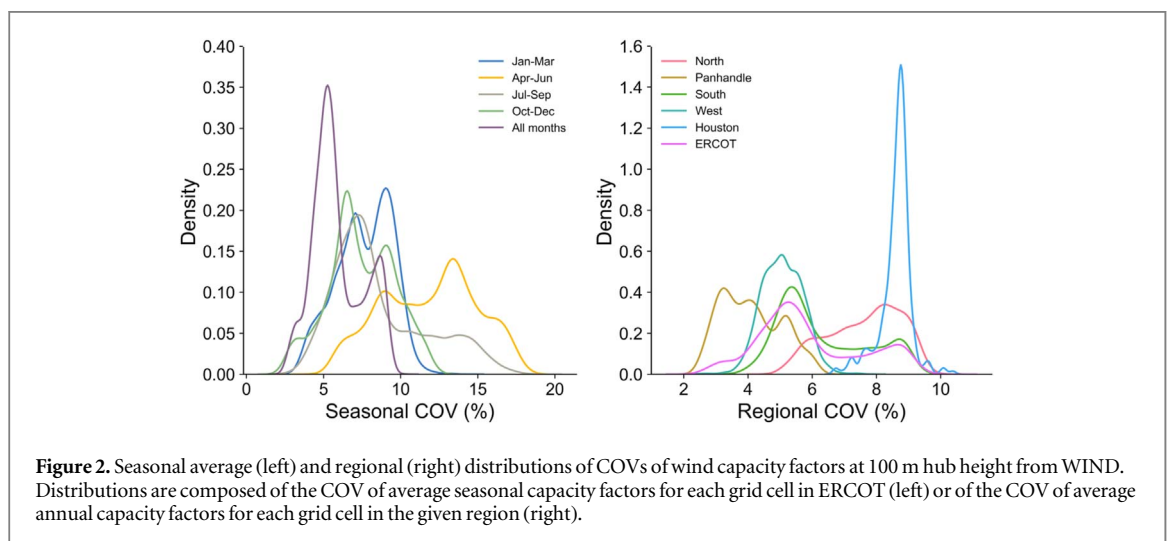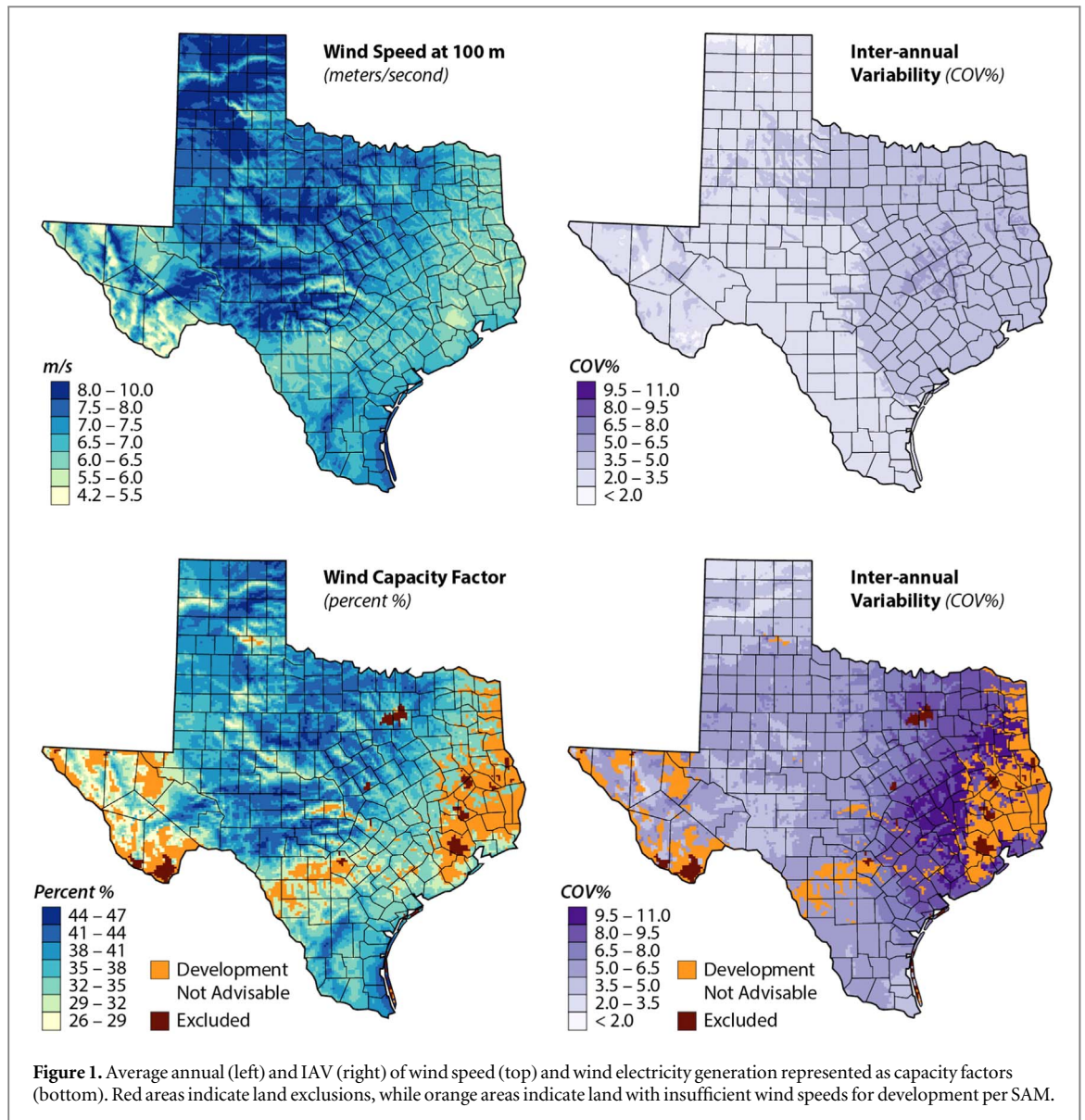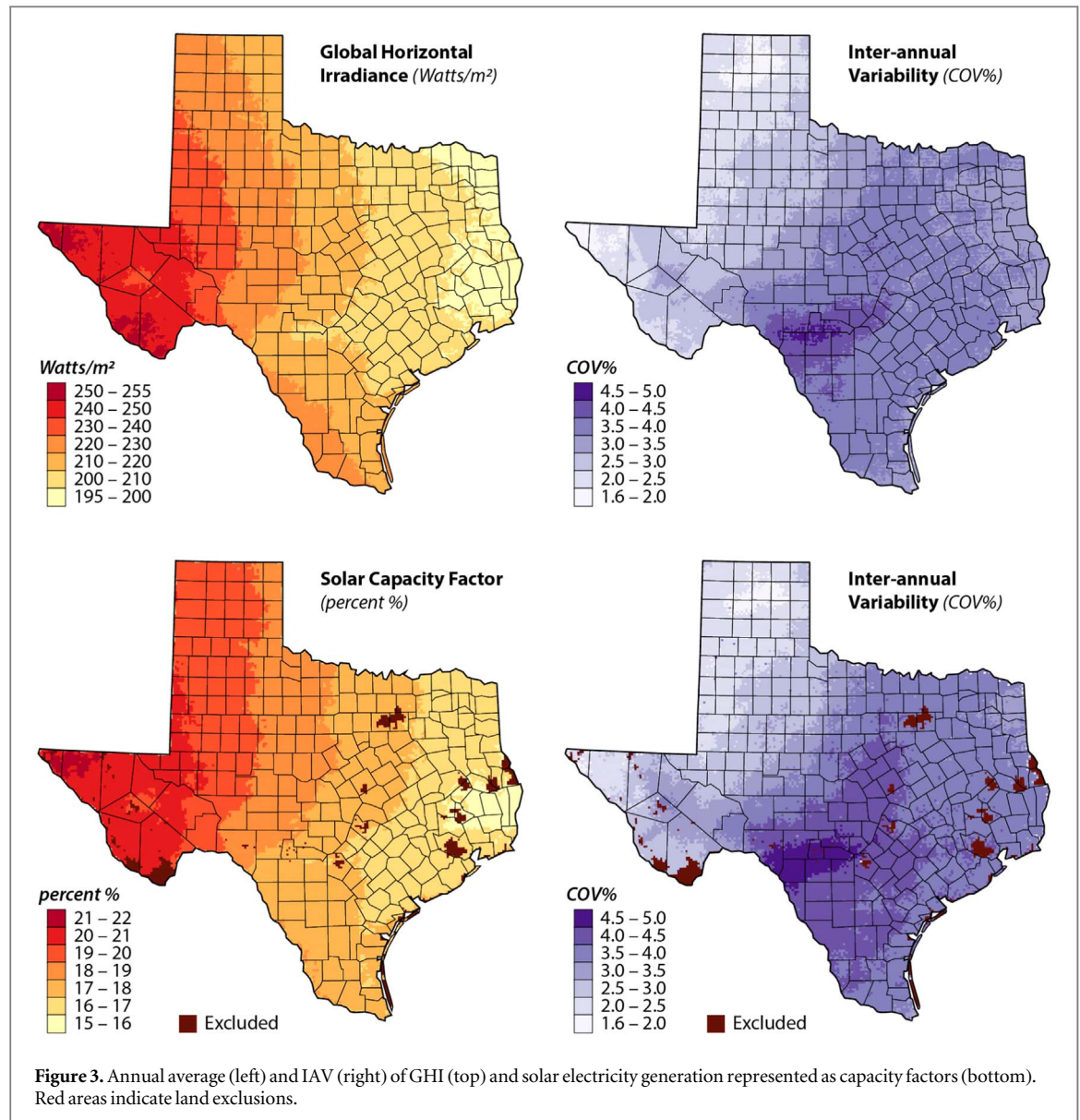
3.2. IAV of solar resource and generation
3.2.1. Comparing GHI from NSRDB to reanalysis datasets and observations
Like the WIND Toolkit, the NSRDB provides a fair representation of GHI IAV based on reanalysis data (SI.6). The COV for GHI in NSRDB equals 2.9%, slightly greater than that in the reanalysis datasets (2.0%–2.6%). The range of annual average GHI in the NSRDB ($207–233 \, \mathrm{W \, m^{-2}}$), though, is similar to that in ERA-I ($211–236 \, \mathrm{W \, m^{-2}}$) and MERRA-1 ($206–232 \, \mathrm{W \, m^{-2}}$). MERRA-2 and NARR systematically overestimate GHI relative to NSRDB, resulting in a higher range of annual average GHIs in those two datasets. Based on monthly average GHI, the NSRDB also reproduces observed GHI from *in situ* data at Edinburg fairly accurately (SI.6) (Sengupta *et al* 2018).

3.2.2. Spatial and temporal variability of average and IAV of solar resource and generation
To understand the IAV of solar resource and generation across ERCOT, we calculate the annual COV of both for each ERCOT grid cell, ignoring whether that

Figure 1. Average annual (left) and IAV (right) of wind speed (top) and wind electricity generation represented as capacity factors (bottom). Red areas indicate land exclusions, while orange areas indicate land with insufficient wind speeds for development per SAM.

Figure 2. Seasonal average (left) and regional (right) distributions of COVs of wind capacity factors at 100 m hub height from WIND. Distributions are composed of the COV of average seasonal capacity factors for each grid cell in ERCOT (left) or of the COV of average annual capacity factors for each grid cell in the given region (right).

Figure 3. Annual average (left) and IAV (right) of GHI (top) and solar electricity generation represented as capacity factors (bottom). Red areas indicate land exclusions.
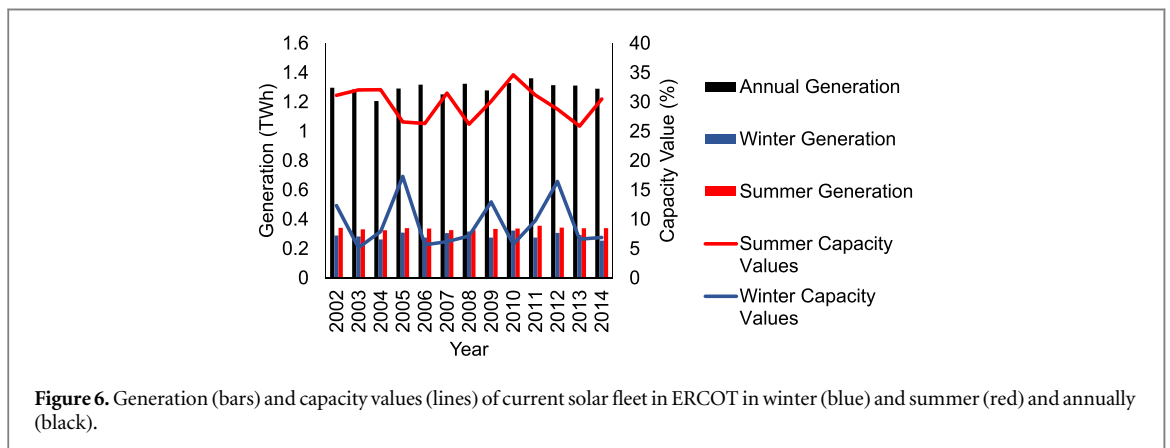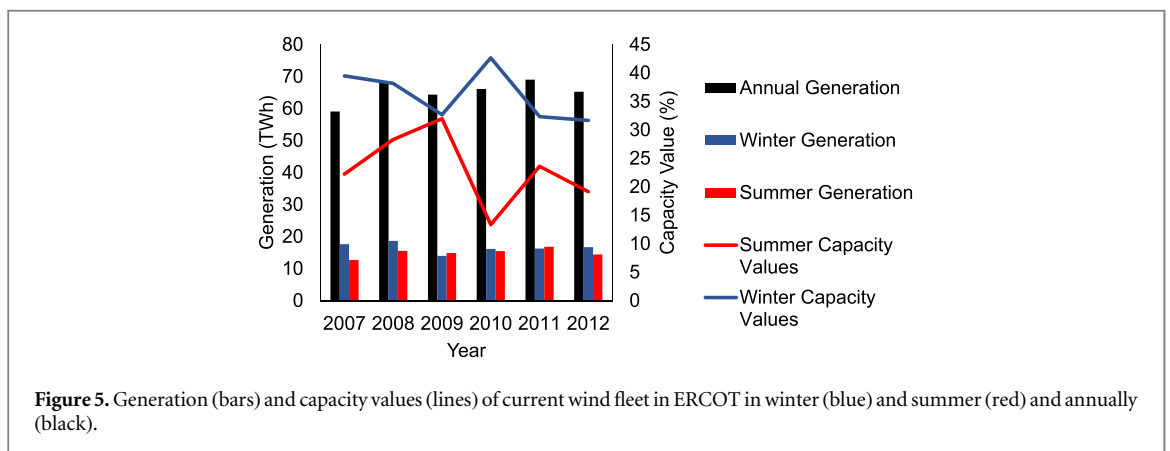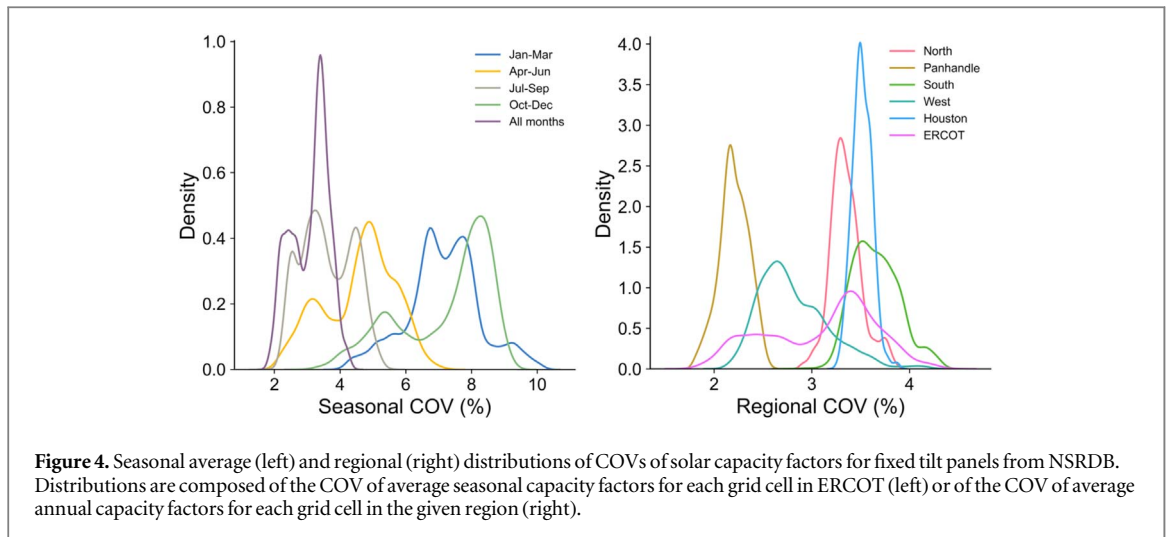
cell currently contains wind and solar generators. Average annual solar resource (represented by GHI) and generation (represented by capacity factors) have similar spatial distributions, with GHI and capacity factors decreasing from high to moderate values from west to east Texas (figure 3). Higher GHI and capacity factors largely coincide with lower IAV, with capacity factor COVs ranging from 2% to 4% from west to east Texas. Defying this trend, though, IAV of GHI and capacity factor is greatest in southwest Texas where GHI and capacity factors are moderate, potentially due to changes in terrain affecting local weather conditions. The mean and standard deviation of the resource and generation are large contributors to how solar COV varies (SI.9). The same cannot be said for wind (SI.9). The COV of solar generation (1.7%–5%) is less than that of wind generation (2.3%–11%), as GHI has a linear relationship with solar generation but wind speed has a cubic relationship with wind generation.

As with wind generation, average annual solar generation IAV exhibits significant seasonal and regional variability (figure 4). Across seasons, the median COV for solar generation ranges from 3.5% in the summer to 7.8% in the fall, with winter and spring falling in between. Median COVs in each season are greater than the median COV across seasons (3.3%), underscoring the importance of temporal resolution when discussing IAV. Significant spatial heterogeneity exists across ERCOT within a season, with fall and winter exhibiting the greatest spatial heterogeneity in COV of roughly 6 percentage points.

Across regions, the median COV for annual average solar generation varies from 2.2% in the Panhandle to 3.6% in the South region. While the Houston region has little spatial variability in COVs due to its small size, large regions like the North and Panhandle also have little spatial variability. In the aggregate, IAV in ERCOT exhibits a bi-modal distribution, mirroring the two clusters of regional distributions and suggesting solar resources

Figure 4. Seasonal average (left) and regional (right) distributions of COVs of solar capacity factors for fixed tilt panels from NSRDB. Distributions are composed of the COV of average seasonal capacity factors for each grid cell in ERCOT (left) or of the COV of average annual capacity factors for each grid cell in the given region (right).

Figure 5. Generation (bars) and capacity values (lines) of current wind fleet in ERCOT in winter (blue) and summer (red) and annually (black).

Figure 6. Generation (bars) and capacity values (lines) of current solar fleet in ERCOT in winter (blue) and summer (red) and annually (black).

in ERCOT could be divided into two classes based on IAV. Using 1-axis tracking rather than fixed tilt panels has little effect on regional and seasonal IAV distributions (SI.10).

3.3. IAV of annual generation and capacity values of current ERCOT wind and solar fleet
3.3.1. IAV of generation by current wind and solar fleet
Given differing system operations and wind and solar resource IAV across seasons, we quantify IAV of wind and solar generation annually and in the winter and

summer for the current wind and solar fleet (figures 5 and 6). From 2007 through 2013, annual wind generation has a COV of 4.8%, less than we calculated when averaging across ERCOT (figure 2), because most wind is installed in the Panhandle, Northwest, and South (SI.1), regions with lower IAV and higher resource quality (figures 1 and 2). Wind generation COV is greater in the summer (8.7%) and winter (8.3%) than annually, confirming our prior ERCOT-wide results of higher seasonal than annual IAV (figure 2). Given that summer and winter are high load

seasons in ERCOT, increased IAV in those seasons could result in large inter-annual dispatch changes. Year-over-year changes in wind generation can be significant. On an annual basis, wind generation averages 65.3 TWh but ranges from 59.6–69.9 TWh, a 17% increase from minimum to maximum (figure 5). Larger increases from minimum to maximum generation occur in the winter and summer of 21% and 33%, respectively.

Contrary to our results when comparing all ERCOT resources (figures 1 and 3), solar generation has a similar COV (4.8%) as wind generation (4.8%) for the current ERCOT fleet. Current ERCOT solar installations are largely not in regions with the highest resource and lowest IAV, potentially due to prioritization of interconnection locations, resulting in a larger COV for annual solar generation than our median estimate based on ERCOT-wide resources of roughly 3.2% (figure 4). Solar generation COV is greater in the winter (7.6%) and smaller in the summer (2.9%) than annually (4.8%), reflecting seasonal differences in cloud cover and GHI. Furthermore, summer solar generation has a narrower range (0.45–0.50 TWh, a 12% difference) than winter (0.24–0.31, a 29% difference) or annual (1.37–1.65 TWh, a 20% difference) generation (figure 6), confirming our prior ERCOT-wide results (figure 4).

3.3.2. IAV of capacity value of current wind and solar fleet

Summer and winter wind capacity values vary significantly across years, with COVs of 28.5% and 12.6%, respectively (figure 5). Winter capacity values range from 32%–43%, a 34% difference, whereas summer capacity values range from 13%–32%, a 146% difference. Thus, wind capacity values have lower IAV in the winter than summer. Furthermore, winter capacity values are larger in each year and on average (36%) greater than summer capacity values (23%). Over our limited timespan, winter and summer capacity values seem to be inversely correlated; from 2009–2010, for instance, summer capacity values decrease by 60% (from 32%–13%), while winter capacity values increase by 24% (from 33%–43%). Additionally, we found no correlation between summer generation and capacity values ($R = 0.06$) and a modest correlation between the two in the winter ($R = 0.41$).

Solar capacity values differ significantly between seasons, averaging 9.3% and 29.8% in the winter and summer, respectively, and with minimum values of 5.2% and 25.9% (figure 6). Furthermore, IAV of solar capacity values are smaller in the summer (9.3%) than winter (45.1%). Lower capacity value IAV in the summer than winter reflects lower generation IAV in the summer than winter. Higher capacity values in summer than winter are due to better solar resource in the summer as well as peak-load hours occurring during daylight hours more often (in the winter, peak load frequently occurs after 7 p.m. in ERCOT). Capacity values are not correlated with generation in the summer ($R = -0.02$) but weakly correlated in the winter ($R = 0.17$), opposite our findings for wind.

When checking resource adequacy, ERCOT assigns capacity values of 59%, 14%, and 75% to coastal wind, non-coastal wind, and utility-scale solar, respectively, in the summer and 42%, 20%, and 9.8%, respectively, in the winter (Electric Reliability Council of Texas 2017c). Because the capacity value is meant to convey the contribution of a resource toward meeting the peak demand over a long-term time frame, the minimum capacity value of our study period is most appropriate for comparison. Our results agree with ERCOT's assigned capacity values for wind and solar during the winter months, but we find smaller capacity values for wind and solar than what is used by ERCOT in the summer (SI.11).

4. Discussion

To better understand how wind and solar IAV may affect system planning and operations, we quantified IAV of wind and solar resource and generation in the ERCOT region while accounting for spatial and temporal variability. We find IAV of solar resource (GHI) and generation are comparable across ERCOT, but due to the cubic relationship of wind speed to wind generation, IAV of wind generation is larger than that of wind speed. Additionally, IAV of wind and solar generation varies significantly across seasons and regions. For instance, the COV for solar generation differs by more than a factor of two between summer and winter and the COV for wind generation differs by a similar amount between the Panhandle and North regions. Furthermore, IAV of wind and solar generation is greater at the seasonal than annual scale, underscoring the need to quantify IAV at sub-annual timescales.

Given high wind and growing solar penetrations in ERCOT and to apply our analysis to a real-world system, we quantified IAV in electricity generation and capacity values of the current ERCOT wind and solar fleet. We found moderate IAV in annual wind and solar generation, which had COV values of roughly 5%. Since wind has been deployed thus far in ERCOT in regions with high resource and low IAV, the COV of wind generation of the actual ERCOT fleet is less than that of all potential wind generation sites. For solar generation, though, the opposite is true, underscoring the need to quantify IAV of actual or expected generator fleets. Capacity values exhibited significantly greater IAV than generation, especially in the summer for wind and winter for solar. This suggests IAV may pose a greater challenge to planning than operations in high renewable systems.

IAV in wind and solar electricity generation could impact power system operations. On an annual,

region-wide basis, IAV in wind and solar generation will affect generation by other fuel types, which in turn can have system- and plant-level ramifications. At the system level, IAV in wind and solar generation will induce IAV in system costs and emissions, potentially leading to missed emission reduction targets in certain years. At the plant-level, IAV in wind and solar generation could affect future revenues, with implications for financing and construction decisions. For example, if a wind plant's first few years of operation are less windy than the long-term average, that can strain project owners' ability to service debts. High IAV can also increase financing rates. IAV in wind and solar capacity values could impact power system planning. If one were to use an average rather than minimum summertime capacity value in doing a planning study, the capacity contribution of wind and solar would be overestimated by 1.9 and 0.3 GW, respectively, resulting in a potential combined capacity shortfall of 2.2 GW. As ERCOT continues to decarbonize, the importance of IAV in planning and operations will increase, as wind and solar will play an increasing role in meeting peak demand and account for an increasing share in annual total generation.

Our results indicate that typical meteorological years (TMYs), or composites of multiple time series that represent average meteorological conditions (Bryce *et al* 2018), should be used with caution in power system studies. While TMY can provide good initial insights, ignoring IAV can lead to skewed results when analyzing high renewable grids. For instance, TMY does not capture years where wind and solar capacity values may be smaller than average, potentially resulting in underinvestment in capacity in planning studies. To obviate this concern, resource planning models might use multiple years of resource data (Shaner *et al* 2018) or select a 'worse' year for evaluating renewable energy capacity value. While small errors in capacity values might have little impact on overall capacity planning results, large misestimates can lead to significant changes in capacity buildout and anticipated costs (Zhou *et al* 2018). More sophisticated probabilistic models (Dent *et al* 2016) can be used to validate planning model results.

Significant room for future research on IAV of wind and solar exists. First, future research should incorporate wind and solar IAV into production cost and capacity expansion models to directly quantify how IAV may affect operations and planning, respectively. Embedding IAV into a capacity expansion model, for instance, would indicate over-build requirements to compensate for capacity value IAV. Second, future research should assess different methods to mitigate wind and solar IAV, particularly of capacity values. Options include grid-scale storage, demand response, and conventional peaking units. Third, studies indicate that climate change might affect wind and solar resources (Haupt *et al* 2016, Karnauskas *et al* 2018), but how it might affect wind

and solar variability is still largely unknown (Tobin *et al* 2016). Future research should quantify how climate change may affect wind and solar IAV, especially given ongoing shifts to high renewable systems.

5. Conclusions

In summary, caution is advised when integrating increasingly larger amounts of wind and solar generation without considering their IAV. We documented differing IAV of wind and solar generation across space and time, and higher IAV in capacity values than annual generation. In the near-term, annual generation IAV will likely need to be compensated for by conventional generators, increasing operational costs and emissions. Due to IAV in wind and solar capacity values, using an average capacity value for wind and solar in planning models can lead to underbuilt power systems, potentially leading to dropped load or reserve shortfalls.

Acknowledgments

ORCID iDs

Andrew Kumler ⓘ https://orcid.org/0000-0002-1533-2193
Michael T Craig ⓘ https://orcid.org/0000-0002-3031-5041
Carlo Brancucci ⓘ https://orcid.org/0000-0002-3605-6730

References

Bañuelos-Ruedas F, Angeles-Camacho C and Rios-Marcuello S 2010 Analysis and validation of the methodology used in the extrapolation of wind speed data at different heights *Renew. Sustain. Energy Rev.* **14** 2383–91

Barbose G, Darghouth N, Millstein D, Cates S, DiSanti N and Widiss R 2016 *Tracking the Sun IX: The Installed Price of Residential and Non-Residential Photovoltaic Systems in the United States* LBNL-1006036 Lawrence Berkeley National Laboratory

Blair N, Dobos A P, Freeman J, Neises T, Wagner M, Ferguson T, Gilman P and Janzou S 2014 *System Advisor Model, SAM 2014.1.14: General Description* US Department of Energy (https://doi.org/10.2172/1126294)

Brower M, Lledó L and Dubois J M B 2013 A Study of Wind Speed Variability using Global Reanalysis Data (AWS Truepower) (https://aws-dewi.ul.com/assets/A-Study-of-Wind-Speed-Variability-Using-Global-Reanalysis-Data2.pdf)

Bryce R, Losada I, Hodge B and Martinez-anido C B 2018 Consequences of neglecting the interannual variability of the solar resource: a case study of photovoltaic power among the Hawaiian Islands *Sol. Energy* **167** 61–75

Carreno I L, Craig M T, Rossol M, Ashfaq M, Batibeniz F, Haupt S E, Ammann C, Draxl C, Hodge B-M and Brancucci C Potential impacts of climate change on wind and solar electricity generation in Texas (in preparation)

Cole W *et al* 2017 *Variable Renewable Energy in Long-Term Planning Models: A Multi-Model Perspective* US Department of Energy (https://doi.org/10.2172/1416124)

Cole W, Frazier A, Donohoo-Vallett P, Mai T and Das P 2018b *2018 Standard Scenarios Report: A U.S. Electricity Sector Outlook* US Department of Energy (https://doi.org/10.2172/1481848)

Cole W, Frew B, Gagnon P, Reimers A, Zuboy J and Margolis R 2018a Envisioning a low-cost solar future: exploring the potential impact of achieving the SunShot 2030 targets for photovoltaics *Energy* **155** 690–704

Davy R J and Troccoli A 2012 Interannual variability of solar energy generation in Australia *Sol. Energy* **86** 3554–60

Dee D P *et al* 2011 The ERA-Interim reanalysis: configuration and performance of the data assimilation system *Q. J. R. Meteorol. Soc.* **137** 553–97

Deetjen T A, Rhodes J D and Webber M E 2017 The impacts of wind and solar on grid flexibility requirements in the electric reliability council of texas *Energy* **123** 637–54

Dent C J, Sioshansi R, Reinhart J, Wilson A L, Zachary S, Lynch M, Bothwell C and Steele C 2016 Capacity value of solar power: report of the IEEE PES task force on capacity value of solar power *2016 Int. Conf. Probabilistic Methods Appl. to Power Syst. PMAPS 2016—Proc.* (Piscataway, NJ: IEEE) (https://doi.org/10.1109/PMAPS.2016.7764197)

Draxl C, Clifton A, Hodge B-M and McCaa J 2015a *Overview and Meteorological Validation of the Wind Integration National Dataset toolkit* US Department of Energy (https://doi.org/10.2172/1214985)

Draxl C, Hodge B, Clifton A and McCaa J 2015b Overview and Meteorological Validation of the Wind Integration National Dataset Toolkit (http://osti.gov/scitech)

Eerme K 2012 Interannual and intraseasonal variations of the available solar radiation *Solar Radiation* (London: IntechOpen) (https://doi.org/10.5772/36137)

Electric Reliability Council of Texas 2017a About ERCOT *ERCOT.com* (http://ercot.com/about)

Electric Reliability Council of Texas 2017b *ERCOT nodal protocols: section 3: Management activities for the ERCOT system*

Electric Reliability Council of Texas 2017c *Report on the capacity, demand and reserves (CDR) in the ERCOT region, 2018–2027* (http://www.ercot.com/content/wcm/lists/143977/CapacityDemandandReserveReport-Dec2017.xlsx)

Electric Reliability Council of Texas 2017d Seasonal Assessment of Resource Adequacy for the ERCOT Region (SARA): Summer 2017

Electric Reliability Council of Texas 2018a *Generator interconnection status report, February 2018* (http://ercot.com/content/wcm/lists/143978/GIS_REPORT__February_2018.xlsx)

Electric Reliability Council of Texas 2018b Hourly load data archives *ERCOT.com*

European Centre for Medium-Range Weather Forecasts 2009 *ERA-Interim Project* Research Data Archive at the National Center

for Atmospheric Research, Computational and Information Systems Laboratory (https://doi.org/10.5065/D6CR5RD9)

Gami D, Sioshansi R and Denholm P 2017 Data challenges in estimating the capacity value of solar photovoltaics *IEEE J. Photovoltaics* **4** 1065–73

Gelaro R *et al* 2017 The modern-era retrospective analysis for research and applications, version 2 (MERRA-2) *J. Clim.* **30** 5419–54

Global Modeling and Assimilation Office (GMAO) 2008a tavg1_2d_rad_Nx: MERRA 2D IAU Diagnostic, Radiation Surface and TOA, Time Average 1-hourly V5.2.0 (Greenbelt, MD) Goddard Earth Sciences Data and Information Services Center (GES DISC) (https://doi.org/10.5067/RI9VTUQN74XJ)

Global Modeling and Assimilation Office (GMAO) 2008b tavg1_2d_slv_Nx: MERRA 2D IAU Diagnostic, Single Level Meteorology, Time Average 1-hourly V5.2.0 (Greenbelt, MD) Goddard Earth Sciences Data and Information Services Center (GES DISC) (https://doi.org/10.5067/B6DQZQLSFDLH)

Global Modeling and Assimilation Office (GMAO) 2015a MERRA-2 tavg1_2d_slv_Nx: 2d,1-Hourly,Time-Averaged,Single-Level,Assimilation,Single-Level Diagnostics V5.12.4 (Greenbelt, MD) Goddard Earth Sciences Data and Information Services Center (GES DISC)(https://doi.org/10.5067/VJAFPLI1CSIV)

Global Modeling and Assimilation Office (GMAO) 2015b MERRA-2 tavg1_2d_rad_Nx: 2d,1-Hourly,Time-Averaged,Single-Level,Assimilation,Radiation Diagnostics V5.12.4 (Greenbelt, MD) Goddard Earth Sciences Data and Information Services Center (GES DISC) (https://doi.org/10.5067/Q9QMY5PBNV1T)

Gueymard C A and Wilcox S M 2011 Assessment of spatial and temporal variability in the US solar resource from radiometric measurements and predictions from models using ground-based or satellite data *Sol. Energy* **85** 1068–84

Haupt S E, Copeland J, Cheng W Y Y, Zhang Y, Ammann C and Sullivan P 2016 A method to assess the wind and solar resource and to quantify interannual variability over the United States under current and projected future climate *J. Appl. Meteorol. Climatol.* **55** 345–63

Holt E and Wang J 2012 Trends in wind speed at wind turbine height of 80 m over the contiguous united states using the north american regional reanalysis (NARR) *J. Appl. Meteorol. Climatol.* **51** 2188–202

International Electrotechnical Commission 2005 International Electrotechnical Commission. IEC 61400-1: wind turbines—Part 1: Design requirements (https://webstore.iec.ch/publication/5426#additionalinfo)

Kaltschmitt W and Wiese A M S 2007 *Renewable Energy: Technology, Economics and Environment* (Berlin: Springer) (https://doi.org/10.1007/3-540-70949-5)

Karnauskas K B, Lundquist J K and Zhang L 2018 Southward shift of the global wind energy resource under high carbon dioxide emissions *Nat. Geosci.* **11** 38–43

Lazard 2017 *Lazard's Levelized Cost of Energy Analysis—Version 11.0* (www.lazard.com/media/450337/lazard-levelized-cost-of-energy-version-110.pdf)

Lew D *et al* 2013 *The Western Wind and Solar Integration Study Phase 2* US Department of Energy (https://doi.org/10.2172/1220243)

Li X, Zhong S, Bian X and Heilman W E 2010 Climate and climate variability of the wind power resources in the Great Lakes region of the United States *J. Geophys. Res.* **115**

Loftus P J, Cohen A M, Long J C S and Jenkins J D 2015 A critical review of global decarbonization scenarios: what do they tell us about feasibility? *WIREs Clim. Chang.* **6** 93–112

Lohmann S, Schillings C, Mayer B and Meyer R 2006 Long-term variability of solar direct and global radiation derived from ISCCP data and comparison with reanalysis data *Solar Energy* **80** 1390–401

Lopez A, Roberts B, Heimiller D, Blair N and Porro G 2012 *U.S. Renewable Energy Technical Potentials: A GIS-Based Analysis* US Department of Energy (https://doi.org/10.2172/1047328)

Madaeni S H, Sioshansi R and Denholm P 2013 Estimating the capacity value of concentrating solar power plants: a case study of the southwestern united states *IEEE Trans. Power Syst.* **28** 1205–15

Markovic M, Jones C G, Winger K and Paquin D 2009 The surface radiation budget over North America: gridded data assessment and evaluation of regional climate models *Int. J. Climatol.* **29** 2226–40

Mesinger F *et al* 2006 North American regional reanalysis *Bull. Am. Meteorol. Soc.* **87** 343–60

Mileva A, Johnston J, Nelson J H and Kammen D M 2016 Power system balancing for deep decarbonization of the electricity sector *Appl. Energy* **162** 1001–9

Milligan M, Frew B, Ibanez E, Kiviluoma J, Holttinen H and Söder L 2017 Capacity value assessments of wind power *Wiley Interdiscip. Rev. Energy Environ.* **6** 1–15

National Centers for Environmental Prediction/National Weather Service/NOAA/U.S. Department of Commerce 2005 NCEP North American Regional Reanalysis (NARR) (Research Data Archive at the National Center for Atmospheric Research, Computational and Information Systems Laboratory) (http://rda.ucar.edu/datasets/ds608.0)

Olauson J and Bergkvist M 2015 Modelling the Swedish wind power production using MERRA reanalysis data *Renew. Energy* **76** 717–25

PJM Interconnect 2017 *PJM manual 21: Rules and procedures for determination of generating capacity. Revision 12* (https://pjm.com/~/media/documents/manuals/m21.ashx)

Pozo-Vázquez D, Wilbert S, Gueymard C, Alados-Arboledas L, Santos-Alamillos F and Granados-Munoz M 2011 Interannual variability of long time series of DNI and GHI at PSA, Spain *Proc. SolarPACES Conf. (Granada, Spain)*

Ramos J and Andreas A 2011 *University of Texas Panamerican (UTPA): Solar Radiation Lab (SRL); Edinburg, Texas (Data); NREL Report* No. DA-5500-56514 University of Texas Panamerican Solar Radiation Lab (https://doi.org/10.5439/1052555)

Ribera T *et al* 2015 *Pathways to deep decarbonization—2015 report INIS-FR–16-0085* International Atomic Energy Agency (IAEA) (https://inis.iaea.org/search/search.aspx?orig_q=RN:47006496)

Rienecker M *et al* 2011 MERRA: NASA's modern-era retrospective analysis for research and applications *J. Clim.* **24** 25

Rose S and Apt J 2015 What can reanalysis data tell us about wind power? *Renew. Energy* **83** 963–9

Sengupta M, Xie Y, Lopez A, Habte A, Maclaurin G and Shelby J 2018 The national solar radiation data base (NSRDB) *Renew. Sustain. Energy Rev.* **89** 51–60

Shaner M R, Davis S J, Lewis N S and Caldeira K 2018 Geophysical constraints on the reliability of solar and wind power in the United States *Energy Environ. Sci.* **11** 914–25

Skamarock W C, Klemp J B, Dudhia J, Gill D O, Barker D M, Duda M G, Huang X Y, Wang W and Powers J G 2008 A description of the Advanced Reasearch WRF Version 3 *NCAR Technical Note* TN 475+ STR The National Center for Atmospheric Research p 113

Tobin I *et al* 2016 Climate change impacts on the power generation potential of a European mid-century wind farms scenario *Environ. Res. Lett.* **11** 034013

US Department of Energy 2017 Business Energy Investment Tax Credit (ITC) *Energy.gov* (https://energy.gov/savings/business-energy-investment-tax-credit-itc)

US Department of Energy 2018 Renewable electricity production tax credit (PTC) *Energy.gov* (https://energy.gov/savings/renewable-electricity-production-tax-credit-ptc)

US Energy Information Administration 2018 *Electric Power Monthly December 2017* (https://eia.gov/electricity/monthly/archive/february2018.pdf)

US National Renewable Energy Laboratory 2016 Renewable resource data center *NREL.gov* (www.nrel.gov/grid/data-tools.html)

US National Renewable Energy Laboratory 2017 National Solar Radiation Database (NSRDB) *NREL.gov* (https://nsrdb.nrel.gov/)

Wan Y H 2011 *Analysis of Wind Power Ramping Behavior in ERCOT* NREL/TP-5500-49218 National Renewable Energy Laboratory (NREL) (Golden, CO)

Wan Y H 2012 *Long-Term Wind Power Variability* US Department of Energy (https://doi.org/10.2172/1033036)

Wiser R H and Bolinger M 2017 *2016 Wind Technologies Market Report* LBNL-2001042 Lawrence Berkeley National Laboratory

Wiser R, Lantz E, Mai T, Zayas J, Demeo E, Eugeni E, Lin-powers J and Tusing R 2015 Wind vision: a new era for wind power in the United States *Electr. J.* **28** 120–32

Zhao J, Abedi S, He M, Du P, Sharma S and Blevins B 2017 Quantifying risk of wind power ramps in ERCOT *IEEE Trans. Power Syst.* **32** 4970–1

Zhou E, Cole W and Frew B 2018 Valuing variable renewable energy for peak demand requirements *Energy* **165** 499–511